Rheology of dense snow flows
Inferences from steady state chute-flow experiments

Pierre G. Rognon (1,2), François Chevoir (2), Hervé Bellot (1),
Frédéric Ousset (1), Mohamed Naaïm*(1) and Philippe Coussot (2)

1. CEMAGREF, 2 rue de la Papeterie, BP 76, 38402 Saint-Martin d'Hères, France.

2. LMSGC, Institut Navier, 2 allée Kepler, 77 420 Champs sur Marne, France.

23^{rd} March 2007

Abstract

A good knowledge of snow rheology is useful for the mitigation of avalanches. However, experiments with snow are difficult and the few available data provide only a partial knowledge of snow flows. In this study we investigate the rheological behavior of the dense flow of dry snow, which often occurs in real avalanches. To this end, we carried out over three winters systematic small-scale in-situ flows down a flume with natural snow. We performed about a hundred experiments with various slope and flow discharge and we characterized them by the measurements of velocity profile and basal stresses. This data set, unique in its extent, enables us to identify some generic characteristics of dense snow of dry snow which are found to differ from common fluids. We point out that snow flows develop as a very viscous upper thick layer over a much less viscous thin layer. We interpret this heterogeneity as a consequence of a shear-induced evolution of snow microstructure which gives rise to different materials between the lower part made of single snow grains and the upper layer made of large aggregates. We finally show that a single constitutive law which describes dense flow of cohesionless grains can represent the behavior of each layers assuming a different size of grains. Beside its practical importance, this study about snow flow provides new insights into the rheological behavior of similar materials: the wide variety of cohesive granular materials such as humid sand, powders, and bituminous suspensions.

1 Introduction

Snow avalanches cause extensive economic damage in mountainous areas. Understanding of snow flow is crucial for risk mitigation, via a better prediction of hazard zones and the optimization of costly defense structures such as dams and braking mounds. Despite these practical needs, the characteristics of the snow flow are still largely ignored. This is partially due to the strong difficulties inherent in experimenting with snow. But the major obstacle is the complexity of the material: not only does snow belong to the wide variety of cohesive granular materials such as humid sand and powders, but its microstructure evolves in time as function of thermodynamical conditions. As a consequence, snow grains may exhibit various shape, size and cohesive interaction. Gaining new insights into snow flow rheology thus requires identification the interplay between the properties of the flow and the properties of the grains, especially their cohesive interaction.

*mohamed.naaim@cemagref.fr

In this paper we investigate the rheological behavior of dense flow of dry snow. In this end, we carried out over three winters systematic small-scale in-situ flows down a flume with natural snow. Experiment at high altitude is unusual in its logistical complexity, but is necessary to have access to natural snow. We performed about a hundred of flows with various slope and flow discharge, and we characterized them by the measurements of velocity profile and basal stresses. From this extensive database, we identify some generic characteristics of the dense snow of dry snow which are found to differ from common fluids. We interpret this behavior as a consequence of a shear-induced evolution of snow microstructure, and we point out its similarities with the behavior of dense granular flow.

The introduction contains some elements of snow morphology, and reviews the previous experimental studies about dense flow of dry snow. The experimental procedure is detailed in § 2. Snow flow behavior is identified from general observations such as steady and uniform flows and discharge equation in § 3, then from the analysis of the velocity profile in § 4. An interpretation of this behavior is proposed in § 5. Conclusions and perspectives are drawn in § 6. Preliminary results can be found in Bouchet *et al.* (2003); Bouchet (2003); Bouchet *et al.* (2004); Rognon (2006); Rastello07 & Bouchet (2007).

1.1 Different kinds of snow

Snow is a peculiar granular material since the size of the snow grains, their shape and their mechanical properties continuously evolve in time as a function of thermodynamical conditions (Marbouty, 1980; Colbeck, 1983; Brown *et al.*, 2001). This process, referred to as snow metamorphism, gives rise to various kinds of snow grains within the snow covert. They can be roughly classified into three categories. *Fresh snow* corresponds to the ice crystals such as those formed in clouds, with ice branches of few millimeters long, called dendrites, whose tangle gives rises to *felting cohesion* (Nakaya, 1954; Reiter, 2005). However, since the dendrites are weak and easily sublime, fresh snow tend to transform into smaller (0.1 to 0.5 mm) and more spherical grains, referred to as *fine grains*. Then felting cohesion vanishes while sintering forms small ice bonds between grains (Kuroiwa, 1974; Colbeck, 1998). This grain type constitutes the main mass of snow cover under freezing temperature. Under positive temperature both ice bonds and grain surfaces melt, and fine grains transform into larger grains (few millimeters) linked via the *capillary cohesion* of liquid menisci.

Many works focused on the relationship between the macroscopic mechanical behavior of the snow cover and the properties of snow grains (Voitkovsky *et al.*, 1974; St Lawrence & Bradley, 1974; Kry, 1975; Gaméda *et al.*, 1996; Johnson & Schneebeli, 1999; Schweizer & Camponovo, 2001; Lehing *et al.*, 2002; Haenel & Shoop, 2004). In contrast, little is known concerning the interactions of snow grains within a flow. The studies of binary collision between two artificial ice spheres of few centimeters pointed out the dependence of energy dissipation and adhesion on the temperature, and the existence of a thin liquid layer at the surface of grains (Bridges *et al.*, 1984; Hatzes *et al.*, 1988, 1991; Higa *et al.*, 1995; Supulver *et al.*, 1995). However, these large ice spheres strongly differ from natural snow grains which are generally much smaller and porous.

1.2 Experimental knowledge on dense snow rheology

Snow flows properties were investigated through two complementary approaches: artificial triggering and small scale experiments. Several full-scale avalanche test sites provided interesting information concerning velocity and wall stresses of snow avalanches which are useful for engineering purpose (Naaim & Naaim-Bouvet, 2001; Dent & Lang, 1983; Qiu *et al.*, 1997; Dent *et al.*, 1998; Vallet *et al.*, 2001; Meunier *et al.*, 2004). Such studies also lead to the distinction of two types of snow flows, namely *powder flows* and *dense flows*. Powder flows are made of snow grains fluidized in air (with a very low density ~ 1 kg/m^3), and move very fast more and less independently of the relief. In contrast, dense flows (density between 100 and 500 kg/m^3) follow the slope and are made of a continuous network of grains in contact. Natural snow avalanches usually contain a basal dense flow above which a powder flow develops. Although they give

access to crucial informations, full-scale experiments are not controlled and impossible to reproduce, and measurements within flows are difficult to obtain.

Small scale experiments can be much more easily controlled, and are therefore more appropriate for a rheological investigation. The typical approach consists in performing dense snow flow down an inclined channel, either set into a cold room (Nishimura & Maeno, 1989) or at high altitude (Tiefenbacher & Kern, 2004; Kern *et al.*, 2004; Bouchet *et al.*, 2003, 2004), and then analyzing some internal velocity profiles in rheological terms. Despite the strong differences in experimental procedures (channel size, snow preparation, etc), the velocity profiles were found to be remarkably consistent with the velocity profile measured on full-scale avalanches by Gubler (1987); Dent *et al.* (1998): snow flows are strongly sheared in a thin basal layer and much less sheared in the upper thick part. Such a velocity profile evoked the behavior of a yield stress fluid for which the free surface flow over an inclined plane exhibits a plugged region above some critical depth. In this context the Bingham (Nishimura & Maeno, 1989), the Herschel-Bulkley and the Cross models (Kern *et al.*, 2004), and a biviscous model (Dent & Lang, 1983) were used to represent the snow behavior. These models gave rise to satisfactory fits of snow velocity profiles when adjusting a non-null slip velocity at the bottom of the flow. Thus, the existing experimental data suggest that the snow behavior may be described by simple constitutive laws. However, this conclusion is rather partial since it is based on few experiments, and it was not checked if one of these models is able to predict the flow characteristics of snow for different slopes and flow rates.

Since snow is made of grains, several studies indirectly investigated snow avalanche behavior through extensive experiment with granular materials such as glass beads. Friction laws that describe granular flow down an inclined plane (Savage, 1979; Savage & Hutter, 1989; Pouliquen, 1999; Louge & Keast, 2001) are often used into full-scale avalanche simulation using Saint-Venant approach (Naaim *et al.*, 1997; Mangeney *et al.*, 2003). Interaction between granular flow and obstacles provided some scaling laws allowing to the design of efficient defense structures against snow avalanches (see for example Faug *et al.* (2007) and reference therein). Rapid granular chute-flow experiments pointed out the formation of a dilute layer at the free surface of dense flow, that may favor the fluidization of small grains such as snow ones (Barbolini *et al.*, 2005*b*), and also investigated the strong interaction between the flowing material and an erodible bed (Barbolini *et al.*, 2005*a*), a crucial process for snow avalanches (Naaim *et al.*, 2004). However, how the granular flows are similar to the snow flows is still an open question, since the comparison would require many more experiments with natural snow than those existing so far. While granular experiments generally involve cohesionless grains, one can expect that intergranular cohesive force between snow grains play an important role in the rheological properties. And since this cohesion significantly evolve throughout snow metamorphism, it is not clear whether there exists a generic behavior for dry snows

2 Experimental procedure

The snow flows have been performed over 3 years at the experimental in-situ test site situated at the *col du Lac Blanc*, a pass near the Alpe d'Huez ski resort in the French Alps. The high altitude (2830 m) enables the access to large amounts of natural snow between January and April. The set-up and instrumental devices were described in Bouchet *et al.* (2003); Bouchet (2003); Bouchet *et al.* (2004); Rognon (2006).

2.1 Flow geometry and feeding system

The flow geometry is a 10 m long channel (Fig.1 a). Its width and height are 20 cm. The slope can be set from 27° to 45°. In order to avoid wall slip the channel bottom was covered with sand paper with a roughness of the order of the snow grain size ($\sim$ 0.4 mm). In contrast the lateral walls were smooth (PVC) and the material could slip. Effectively our measurements showed that the velocity at the free surface of the flow was almost constant in a cross-section (see Section 4.1), which suggests that the lateral walls negligibly affected the flow characteristics, probably due to wall slip. Actually it was shown by Jop

et al. (2005) that even in that case channelized granular flows can be affected by the lateral walls but taking into account this effect here would not change the conclusions below. Under these conditions we assume that the flow characteristics are those of the flow over an infinitely wide plane and in steady-state the stress distribution may be deduced from the momentum equation (Coussot, 2005).

The feeding system is an important feature of the experimental set-up. It is made of a hopper which can store up to 5 m^3 of snow and an Archimedean screw 4 m long with a 0.6 m diameter. The screw injects the snow into the channel at a constant flow rate which can be adjusted up to 0.1 m^3/s by varying the rotational frequency (up to 1 Hz). Although the flow rate averaged over a period of rotation is constant, it slightly depends on the orientation of the screw, leading to periodical variations of the order of 20%. In order to limit the effect of such variations on the flow characteristics we set up at the beginning of the chute a system that deviates outside the flume the upper part of the flow and thus ensures a constant flow rate downstream.

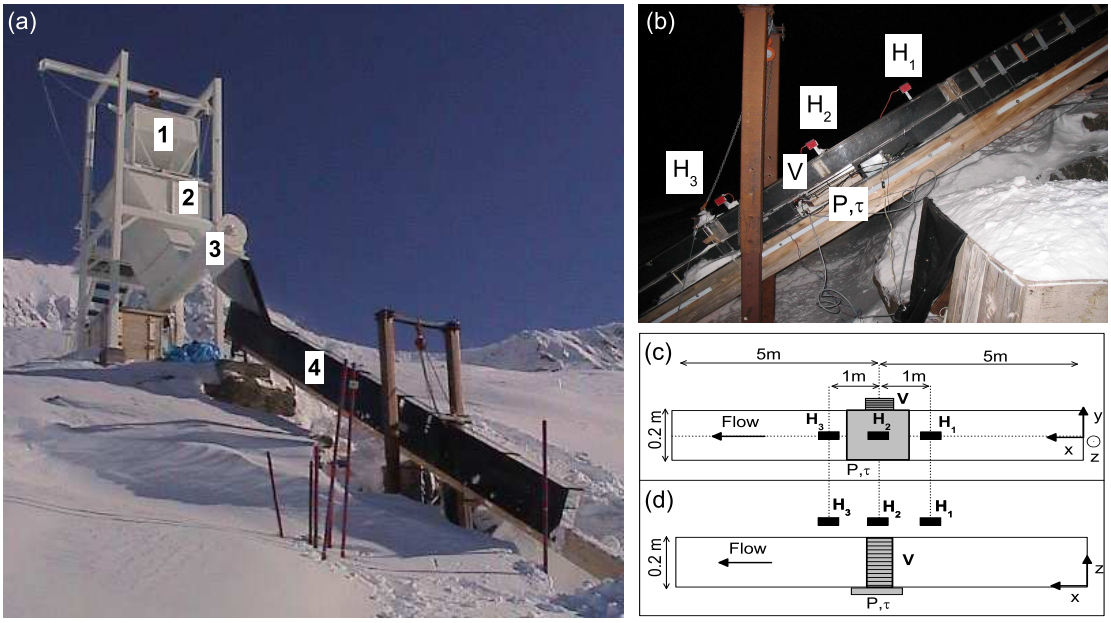

Figure 1: Experimental set-up at the *Col du Lac Blanc* (Alpes d'Huez, 2830m). (a) set-up : (1) moving tank, (2) hopper, (3) Archimedean screw, (4) channel. (b) Position of sensors (flow depth $H_{1,2,3}$, velocity profile V and basal stresses P and τ) : lateral view of the chute, and schematic views (c) from the top, and (d) from the side.

2.2 Measurements

The sensors are set around the middle of the chute (Fig. 1 b-d). They record the flow height H at three points along the flow direction, the normal (P) and shear (τ) stresses at the bottom and the velocity profile $V_x(z)$ along the depth z. The data are recorded during the whole duration of flows with a sampling frequency $\mathcal{F}_{acq}$=10 kHz. The three height sensors (LEUZE ODS M/V-5010-600-421) are fixed above the

channel (z=0.3 m) at y=0. They emit an optical light and detect the position of the beam reflected by the flow. This position gives rise to the flow thickness from 0 to 20 cm with a precision of 1 mm. The stress sensor is a bi-component piezo-electric (Kistler $9601A21 - 2 - 20$) sandwiched between two metal plates of 0.2 m (along the channel width) by 0.5 m. It is inserted into the bottom of the channel and its upper surface is covered with sand paper.

The velocity measurements are based on the correlation of two signals from identical sensors located at two successive positions along the channel (Dent *et al.*, 1998; Bouchet *et al.*, 2003). Each sensor is an optical device which emits an infrared light and measures the intensity of the reflected beam. The corresponding signal is related in a non-trivial way to density, granularity and microstructure of the reflecting snow. Two such devices located at a distance δ=7.2 mm along the flow direction give similar signals $X(t_i)$ and $Y(t_i)$, but shifted by a time $\Delta t(z) = \delta(z)/V_x(z)$ where $V_x(z)$ is the velocity (Fig.2 a). The value of $\Delta t_i(z)$ is the time shift for which the discrete cross correlation function $\mathcal{C}(z)$ between signal $X(t_i, z)$ and $Y(t_i, z)$ reaches its maximum (Fig.2 b). The similarity of the two signals $X(t_i, z)$ and $Y(t_i, z)$ is good if the microstructure of the moving snow is constant, so that the distance δ must be as small as possible. As a counterpart the shift time is small ($\Delta t_i \approx 1.5\ ms$ for a typical velocity of 5 ms^{-1}), and its relative precision $1/\left(\Delta t_i \times \mathcal{F}_{acq}\right) \approx 7\%$ is low. To get a better precision, the discrete correlation function is fitted by a quadratic function including ten points around Δt_i, and Δt is defined as the time shift that peaks this function (Fig.2 b, insert). The apparatus for the velocity profile consists of 13 pairs of sensors stacked along z (Fig.2 c). Then the column is inserted in a lateral wall, setting the bottom of the first sensor at z=0. The sensors are dispatched each centimeter, excepted for the first two centimeters where the spatial resolution is increased (0.5 cm), which requires placing the sensors in two columns.

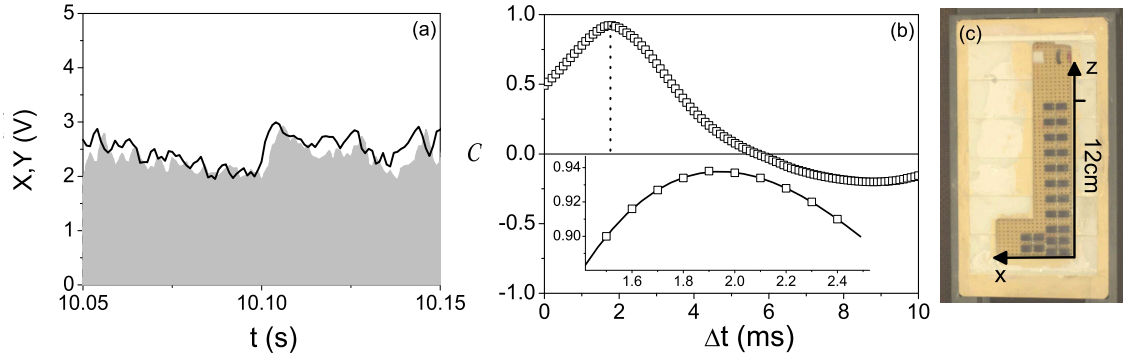

Figure 2: Velocity measurements : (a) typical signals recorded from a pair of optical sensors, (b) cross correlation $\mathcal{C}(\Delta t_i)$ of these signals, inset : quadratic fit around the peaks of $\mathcal{C}(\Delta t_i)$, (c) distribution of sensors.

2.3 Procedure

15 series of experiments were performed over three winters, providing 85 flows (Fig. 3 a). For each series two days were needed to clean up the channel often buried under several meters of snow, install the electronic devices and repair the damages in the mechanical structure caused by the mountain harsh weather. The experiments were performed overnight at temperatures ranging from -25^{circ}C to -3^{circ}C,

which prevents the presence of liquid water. Snow cover was collected nearly and was prepared as a mixture of individual grains (typical diameter ranging from 0.1 to 0.5 mm) or clusters of size smaller than 2 cm by passing it through a grinder. This mixture was then stored in the moving tank. During this operation (which lasted about 20 minutes) the ice grains could sinter and form a solid block inside the moving tank. A few minutes before the beginning of the experiments, the moving tank was emptied into the hopper through a sieve of 3 cm-mesh width, which broke the large snow blocks into a mixture of individual grains and aggregates of diameter smaller than a mesh width. Then the Archimedean screw was activated and the mixture was injected into the channel. Up to ten runs per night could be performed.

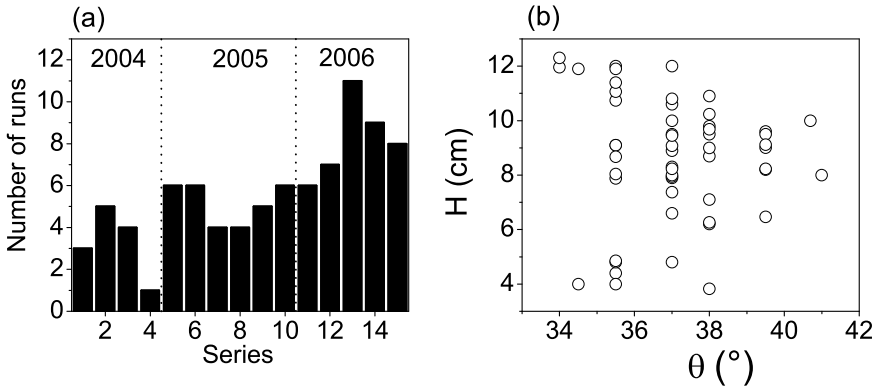

Figure 3: *Details of performed runs : (a) number of runs for each series (the labels inside are the years), (b) ranges of slope θ and flow depth H for which steady uniform flows were obtained.*

3 General properties of flow

We first present the overall characteristics of the snow flows, from the evolution of the mean velocity over the depth, $U = \int_{z=0}^{H} V_x(z)dz$, as a function of the slope and flow discharge.

3.1 Flow regimes

Since the flow rate (Q) imposed by the feeding system is constant during the flow, and neglecting variations of the snow density along the flume axis, the mean velocity (U) in the direction x is readily found from the mass conservation: $U(x) = Q/H(x)$, in which $H(x)$ is the flow height. From the measurements of the flow thickness along the channel axis, we observed three flow regimes depending on the slope angle θ of the flume (Figure 4). For a slope lower than approximately 33°, the flow depth increases downstream, which means that the average velocity U decreases downstream. This corresponds to a *decelerated flow regime*. When the flow decelerates enough, it stops inside the channel and the snow eventually forms a rigid bloc within a few seconds. Afterwards, the snow does not flow any more even when the slope is increased up to 45° (maximum value allowed by the set-up), which means that just after the liquid-solid transition the material viscosity rapidly increases. Conversely, for slopes larger than approximately 41°, the flow depth typically decreases downstream by roughly one centimeter per meter. This corresponds to an *accelerated flow regime*. In that case we observe that the snow grains start to be fluidized at the end

of the flume and the flow appears to be made of a dense layer covered by a cloud of snow grains, a flow type reminiscent of powder snow avalanches.

For intermediate slopes, the flow depth is constant along the channel, so that U is constant too, which corresponds to a *steady and uniform regime*. Various tests leading to such steady, uniform flows were carried out at different slopes in the range 33-41°, and various depths in the range 4-12 cm (Figure 3 b). Figure 5 shows the typical time evolution of the flow parameters for such a steady, uniform flow either directly measured or deduced from measurements. After a short transient phase the three depths along the channel reach similar steady values with some fluctuations around their mean value. This steady state typically lasts for 10 s. The standard deviation of the time fluctuation is around 0.7 cm for each sensor. The normal stress P exerted by the flowing layer on the bottom also reaches a steady value with fluctuations of the order of 10%. The average density of the flow over a cross-section of the channel can be deduced from the simultaneous measurements of P(t) and H(t) with the help of the momentum equation in the direction z: $\bar{\rho} = P/(gH\cos\theta)$. It also reaches a steady-state value with some fluctuations of the order of 10%. Under these conditions the shear stress at the bottom that results from gravity can be deduced from $\bar{\rho}(t)$ and $H(t)$: $\tau_g = \bar{\rho}gH\sin\theta$. We find that the shear stress τ measured at the bottom balances the gravity stress ($|\tau| = \tau_g$), which, using the momentum equation, confirms that the flow is neither accelerated ($|\tau| < \tau_g$) nor decelerated ($|\tau| > \tau_g$), i.e. we are dealing with a steady-state, uniform flow.

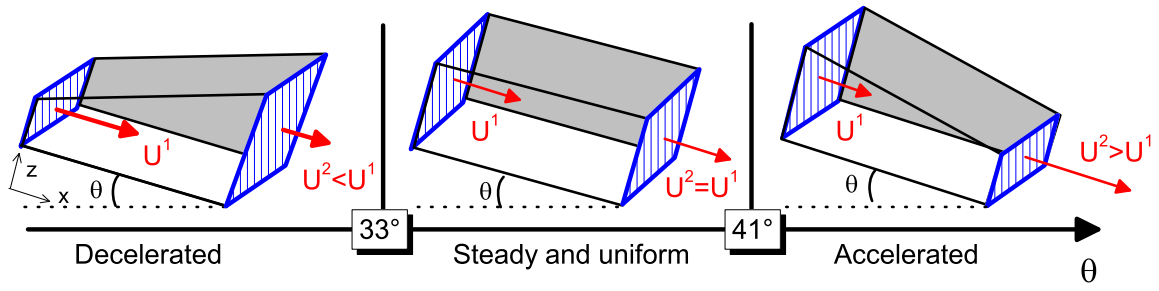

Figure 4: *Scheme of the three flow regimes as function of the slope θ, deduced from flow depth measurements along the flume.*

3.2 Variation of the mean velocity U

Figure 6 plots the mean velocity U of several steady and uniform snow flows either as a function of the slope for similar depths, or as a function of depth for same slopes. The data are remarkably consistent. This is surprising since, due to their continuous metamorphism, the physical characteristics of snow grains differed for all the runs performed at different periods over the three years. This suggests that generic, macroscopic properties of dense snow flow can be identified. More precisely a rheological analysis of these data in terms of flow characteristics only, i.e. without taking into account the different snows, is relevant and should provide some general properties of the snow.

For any simple viscous fluid (Newtonian or power-law), we expect a continuous increase of the average velocity U from zero as the slope angle of the flume is increased. For a yield stress fluid, U is null as long as the slope is lower than a critical value, then continuously increases from zero when the slope is further increased. In contrast, with snow, $U(\theta)$ varies in an unusual way (Figure 6 a): it is equal to zero up to 33° then abruptly takes a slowly increasing value between 3 ms^{-1} and 4 ms^{-1}, for a slope angle

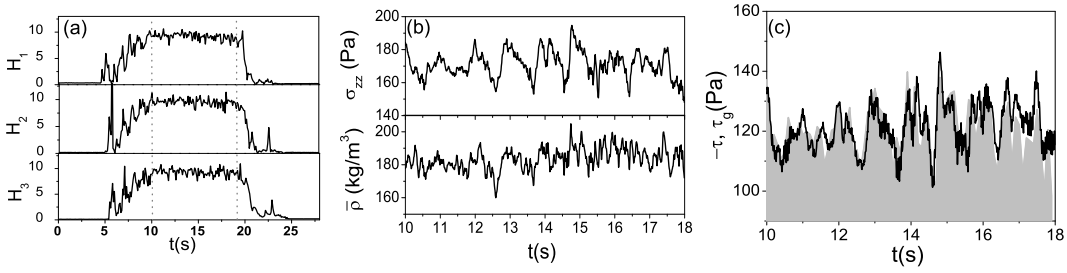

Figure 5: Time evolution of some quantities during a typical steady uniform flow with $\theta = 37°$: (a) flow depths measurements (averaged values: $H_1(t) \approx 9.8$ cm, $H_2(t) \approx 9.5$ cm, $H_3(t) \approx 9.6$ cm), (b) basal normal stress ($P = 170 \pm 10\%$) and deduced average density ($\bar{\rho} = 180 \pm 10\%$), (c) measured basal tangential stress τ (—) and tangential stress deduced from the momentum balance τ_g (gray).

between 34° and 41°. This discontinuity in velocity vs slope is reminiscent of the flow instability observed for colloidal suspensions, which somewhat restructure at rest and start to flow abruptly when the slope reaches a critical value (Coussot *et al.*, 2002). It is also reminiscent of the behavior of granular flows over inclined plane for which it was shown that no uniform flow could take place at an average velocity smaller than a critical value depending on H (Pouliquen & Chevoir, 2002).

Let us now consider the material behavior in the liquid regime (33-41°) for which steady, uniform flows are observed. Steady and uniform flows down inclined are useful for a rheological investigation, since the variation of the mean velocity U vs flow depth H, i.e. the discharge equation, can be related to the constitutive equation of the flowing material, i.e. the relationship between the shear rate $\dot{\gamma}$ and the shear stress (Astarita *et al.*, 1964; Coussot, 2005). In Appendix A, we recall the demonstration that gives rise to:

$$\dot{\gamma}(\tau_g) = \frac{1}{H} \left. \frac{\partial(UH)}{\partial H} \right|_{\theta} . \tag{1}$$

This result holds for any constitutive law, under the assumptions that the flow is steady and uniform and that the sliding velocity is null.

With snow, the mean velocity slightly increases with the flow depth (Figure 6 b). This evolution is linear in the range 4¡H¡12 cm. According to 1, this predicts a decrease of the shear rate $\dot{\gamma}(\tau_g)$ with the inverse of the flow depth H, which corresponds to a material with a resistance to flow decreasing when the shear stress increases. A linear stability analysis, summarized in Appendix B, then strictly demonstrates that no stable flow of a homogeneous material following a behavior in which τ decreases when $\dot{\gamma}$ increases is possible (Coussot, 2005). Hence, the discharge equation does not holds to measure snow constitutive law. This may be due to a non null sliding velocity between snow flow and bottom. But this may also be the consequence of heterogeneous flows which were made of at least two layers with different constitutive equations.

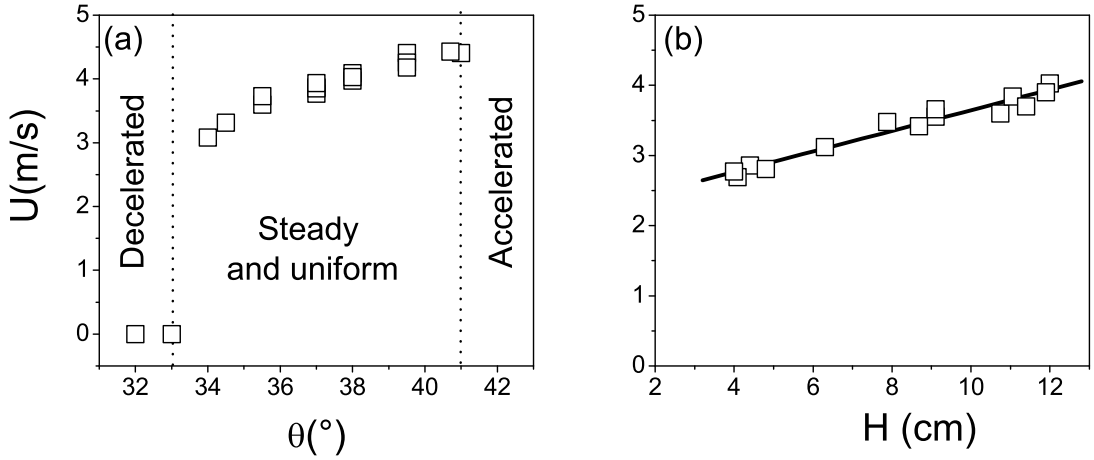

Figure 6: Macroscopic behavior of dense snow flows: mean velocity U for steady and uniform flows performed over three years (a) $U(\theta)$ with $H \approx$10 cm and (b) discharge equation $U(H)$ with $\theta = 35.5°$ and its linear adjustment: $U = 0.02 + 0.15H$ (—).

4 Local behavior

The analysis of the discharge equation is found to be insufficient to determine the constitutive law of the flowing snow, but reveals a possible sliding velocity and/or some structuration of snow flow into layers of different constitutive law. The measurement of the velocity profile inside the flowing layer enable us to refine this conclusion.

4.1 Velocity profiles

4.1.1 Typical velocity profile and lateral wall effect

For the steady, uniform flows, apart from small fluctuations the velocity is constant in time. Figure 7 shows a typical velocity profile $V_x(z)$ as measured during our tests. This velocity profile is qualitatively consistent with the limited previous measurements in a small channel (Nishimura & Maeno, 1989; Bouchet *et al.*, 2004), in a large chute (Tiefenbacher & Kern, 2004; Kern *et al.*, 2004) or within real avalanches (Gubler, 1987; Dent *et al.*, 1998).

Note that our measurements correspond to the velocity along a lateral wall (y=10 cm), which might not well represent the flow behavior elsewhere if there is a significant shear in the transversal direction. The videos of the free surface allow to track some snow aggregates from five successive pictures corresponding to a displacement of about one meter along the flow direction. Their orthogonal velocity is negligible : $V_y^a \approx 0$. The inset of figure 7 shows the velocity of aggregates V_x^a as a function of their transversal position y. The velocity negligibly varies with y, which demonstrates that transversal shear is negligible. Furthermore, figure 7 shows the good agreement between the velocity measured by optical sensors at y=10 cm and the velocity at the flow surface obtained from height correlation at y=0 cm (see sensor location on Fig.1 b). These results support the assumption that the velocity profile $V_x(z)$ measured at the lateral

wall well represents the velocity profile at different transversal positions within the fluid.

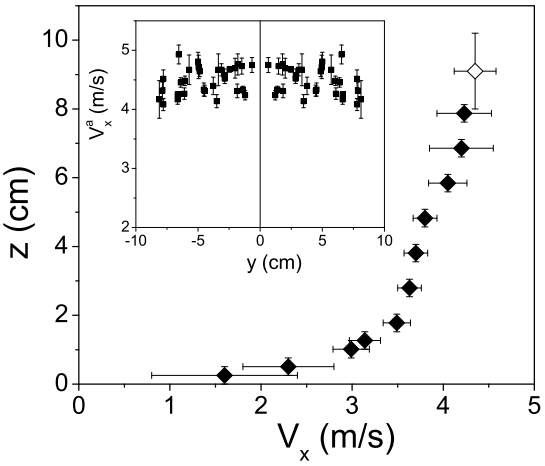

Figure 7: Velocity profile of a typical snow flow ($\theta = 37°$): each point (⧫) corresponds to the time-averaged measurements from one pair of sensor. The horizontal error bars correspond to the associated standard deviation. The vertical error bars represent the width of a sensor. The highest point (◊) was obtained from the correlation between the flow depth measurements performed along the channel. It represents the time-average flow velocity at the free surface, and its vertical error bar corresponds to the standard deviation of the flow thickness over time. The inset shows the velocity V_x^a of aggregates at the free surface as a function of their lateral position y.

4.1.2 Variation of the velocity profiles

Due to the possible material transformation from one run to another, the reproducibility of the experiments is a critical point. We thus repeated some runs keeping constant both the slope and the flow depth. Figure 8 (a) shows that for runs performed over the same night the resulting velocity profiles are similar whereas some variation of about ±15% may be observed for runs performed during nights separated by weeks (Figure 8 b). This indicates that for a given snow (same night, i.e. same series of runs) our initial preparation of the snow is well reproducible, and that the grain transformations within the snow cover during a series of runs do not affect the rheological properties of snow, but they may slightly affect the results from one series to another.

Figure 8 (c) shows the velocity profile for runs performed during the same night with similar depths but various slopes. Conversely, figure 8 (d) shows the velocity profile for runs performed during the same night with the same slope but various depths. For any slope and any flow depth, the velocity profiles exhibit a common type shape: a slightly sheared upper part and a strongly sheared lower part, and although there is no velocity measurement at z=0, an extrapolation of the data in the bottom flow region seems to indicate a non null sliding velocity, about 1 ms^{-1}. We observe that the thickness of the lower part remains almost constant, while the thickness of the upper part increases with the flow depth. The critical point is that although the shear stress is supposed to decrease linearly from the flume bottom the local shear rate (i.e. the slope of the velocity profile) exhibits an abrupt variation at the interface between the two regions (see the inset in figure 8 d). This implies that the flow is heterogeneous: the constitutive law that describes the upper part of the flow cannot describes its lower part. We conclude that both a non-null sliding velocity

and a heterogeneous behavior explain the inconsistency of the analysis attempting to determine a single constitutive law of snow based on the flow discharge equation.

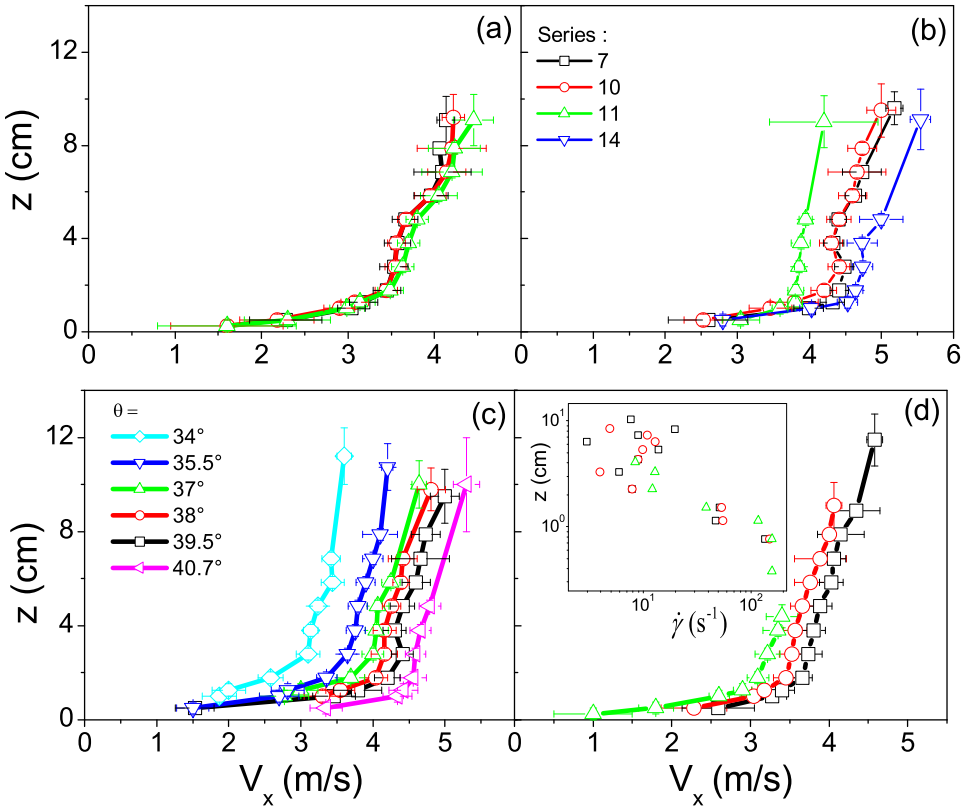

Figure 8: *Variation of the velocity profiles. Reproducibility of the experiment: flows of similar thickness ($H \approx 9$ cm) and same slope ($37°$) (a) performed over the same night, (b) performed over different series spaced by weeks. (c) Effect of the slope: six flows of similar thickness ($H \approx 10.5$ cm) performed over a night. (d) Effect of the thickness: three flows at constant slope ($\theta = 35.5°$) performed over a night; the inset shows the corresponding shear rate at different depths: $\dot{\gamma} = dV_x/dz$.*

4.2 Behavior of each layer

Since the snow flows are made of two layers with different behaviors, we now analyze separately their rheological properties. To this end, we represent the generic form of the velocity profile, a thin, highly sheared basal layer and a much less sheared upper layer, by a simple bilinear function which involves the

characteristic mean shear rates of the top layer ($\dot{\gamma}_u$) and the bottom layer ($\dot{\gamma}_b$), and the thickness of the bottom layer (z_b) (Figure 9):

$$V_x(z) = \begin{cases} \dot{\gamma}_b z & \text{if } 0 < z < z_b, \\ \dot{\gamma}_u z + (\dot{\gamma}_b - \dot{\gamma}_u) z_b & \text{if } z_b < z < H. \end{cases} \quad (2)$$

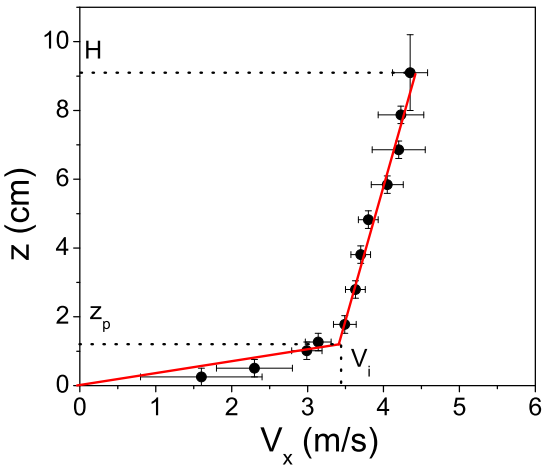

Figure 9: *Typical snow velocity profile with $\theta = 37°$ (•) fitted by the bilinear function of Eqn. 2 (—).*

Such a simple form obviously does not perfectly describe the velocity profiles. First, it leads to a discontinuity of the shear rate at the interface, whereas the data suggest a very rapid but continuous variation. Secondly, while a linear fit is convincing in the upper part, this is not the same in the lower part: the scarce data can be fitted by a curved profile and there might be some non-zero (sliding) velocity along the bottom. However, we do not have enough data in the lower part and they are not sufficiently precise to enable a satisfactory determination of a sliding velocity or a power law for the velocity profile. We therefore content ourselves with describing the behavior of the basal layer using the simple approximation of a linear velocity profile without sliding velocity, and $\dot{\gamma}_b$ represents the averaged shear rate in the bottom layer, including possible wall effect such as sliding.

Nevertheless, the bilinear function 2 represents the main features of the velocity profiles as a first approximation and thereby enables to further analyze the behavior of each layer. Figure 10 shows the variation of the averaged shear rates in both layers, the thickness of the basal layer as a function of the angle with similar flow depth (left column), or as a function of the flow depth with constant slope (right column). For a given flow thickness, both of the shear rates $\dot{\gamma}_b$ and $\dot{\gamma}_n$ increases when the slope θ is increased. However, they differ by one order of magnitude, even tacking into account a sliding velocity about 1 ms^{-1}. Both shear rates slightly decrease when the slope is decreased from 41° to 34°, then brutally drop to zero for 33°. As a consequence the shear rate drops from a critical value ($\dot{\gamma}_c$) to zero at a critical slope θ_c, which may be described in a first approximation as: $\theta - \theta_c \propto \dot{\gamma} - \dot{\gamma}_c$.

Moreover, we observe that the thickness z_b of the basal layer slightly decreases when the shear rate $\dot{\gamma}_b$ is increased. For a given slope, the shear rate in the bottom layer ($\dot{\gamma}_b$) increases with the flow depth, as is expected for any homogeneous flowing material. In contrast, the shear rate in the upper layer $\dot{\gamma}_n$ decreases when H increases. Since the average stress in the layer increases with H, this means that the shear rate decreases when the shear stress is increased. According to the stability analysis mentioned in

section 3.2 (Appendix B), this implies that the constitutive law of the material in the upper layer evolves when the flow depth is varied.

5 Interpretation in terms of rheological model

Snow flows exhibit unusual characteristics that cannot be described by simple viscoplastic models. Some of these characteristics are reminiscent of those of granular flows, and this is not surprising since snow is made of grains. However, data indicate that snow flows are made of two layers which cannot be described by a single constitutive law. We now suggest an interpretation of such a behavior, based on a shear induced evolution of the snow microstructure. Then we check its plausibility using recent advances in the rheology of granular materials.

5.1 Shear-induced evolution of the snow microstructure

The difference of behaviors between the bottom and upper layers may be due to the proximity of the rough bottom which would affect the rheological properties in the basal layer. But it may also by due to a difference of snow microstructure in the two layers. Two visual observations seem to confirm this last interpretation. First, we observe at the end of the flows that several layers of isolated snow grains caught in the asperities of the bed. Secondly, the videos of the free surface reveal the existence of large snow aggregates and allow to measure their emerged size. Figure 11 shows the number N of aggregates of size D throughout a flow.

At the hopper exit, the snow is made of a well mixed mixture of single grains and aggregates of various sizes. Then the two different regions develop as the material moves downwards the flume. The segregation may lead to the formation of these two layers with different size of grains, as it was pointed out with cohesionless granular materials (Savage & Lun, 1988; Khosropour *et al.*, 1997; Rognon *et al.*, 2007). However, we observed that the snow aggregates initially at the free surface remain there all along the flume. According to the low shear rate in the upper part of the flow, this evokes a low agitation state that would not favor the segregation. But another process can give rise to the formation of these layers, as we observed through simulation of cohesive granular flow (Rognon *et al.*, 2006): the lower regions submitted to the largest stresses tend to liquefy, while the upper regions submitted to the smallest stresses tend to gelify. This mechanism corresponds to a kind of viscosity bifurcation, with some similarity with that observed in soft-jammed systems (Coussot *et al.*, 2002). With dry snow, we may expect that the ice bridges between grains cannot resist to the large stresses combined with the grinding process of the bottom roughness, while they are not broken in the upper layer (Fillot *et al.*, 2004). There thus develops a basal layer made of single grains whereas the upper part is made of large aggregates.

5.2 Insights from rheology of granular materials

The composition of snow flow, a mixture of single grains and large aggregates, is reminiscent to a granular material with various size of grains. It is thus tempting to confront the snow behavior with the one of granular material. Although granular rheology is still matter of debate, the two last decades of active researches pointed out many interesting properties. One crucial issue is that granular behavior strongly depends of the solid fraction, and different constitutive laws were proposed to describe either dilute or dense flow. In our situation, the solid fraction within flow is not measured, but can be roughly estimated as the ratio between the density of the flowing snow (about 200 kgm^{-3}) and the density of aggregates, of the order of the density of the snow covert, about 350 kgm^{-3}. According to this estimation, the solid fraction of the flowing snow is around 0.6 which corresponds to a dense configuration where grains interact through multiple maintained contacts, rather than to a dilute configuration with binary collision.

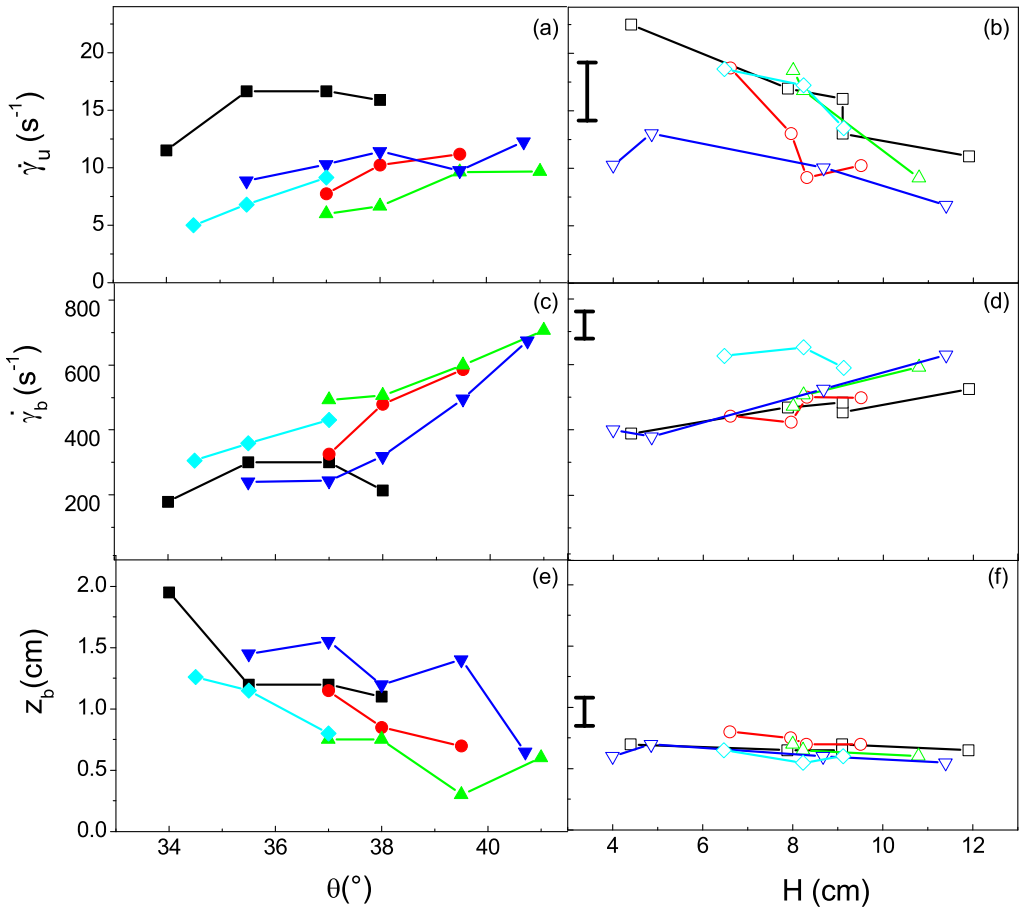

Figure 10: *Rheological properties of the two layers : (a) $\dot{\gamma}_u(\theta)$, (b) $\dot{\gamma}_u(H)$, (c) $\dot{\gamma}_b(\theta)$, (d) $\dot{\gamma}_b(H)$, (e) $z_b(\theta)$, (f) $z_b(H)$. The data are presented as a function of the series of experiments performed over the same night, i.e. with constant properties of snow grains. Flows of similar thickness (left column) : $H \approx 8.5$ cm (▲), $H \approx 10$ cm (●,▼), $H \approx 11.5$ cm (■,♦). Flows of same slope (right column) : $\theta = 37°$ (○,△), $\theta = 35.5°$ (□,▽), $\theta = 38°$ (◊). The uncertainty on the velocity measurements is typically $\Delta(v) \approx 0.5$ ms^{-1}. The uncertainty on the shear rate in the upper layer (thickness ∼0.1 m) may be estimated by $\Delta(\dot{\gamma}_u) \sim \Delta(v)/(0.1m) \sim 5\ s^{-1}$ and the uncertainty on the shear rate in the basal layer (much thinner : ∼ 7 mm) by : $\Delta(\dot{\gamma}_b) \sim \Delta(v)/(7mm) \sim 70\ s^{-1}$. The estimation of the uncertainty on the interfacial velocity $V_i = v(y_b) = \dot{\gamma}_b y_b$ by $\Delta(v)$ allows to deduce the uncertainty on the basal thickness : $\Delta z_b \sim \frac{\Delta V_i}{\dot{\gamma}_b} + \frac{V_i \Delta \dot{\gamma}_b}{\dot{\gamma}_b^2} \sim$ 2 mm.*

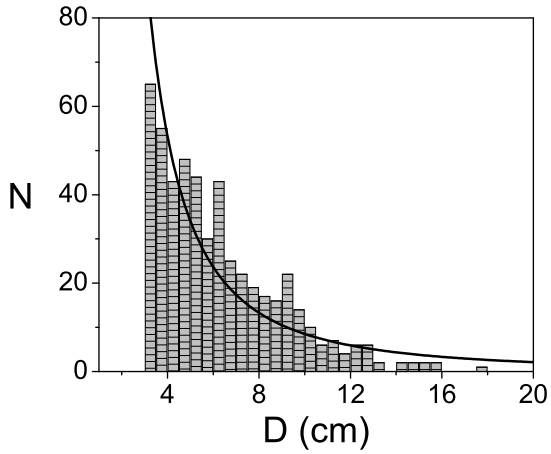

Figure 11: *Size distribution of snow aggregates during steady and uniform flows: measurements from video of the free surface of one flow (bars) and power law* $\frac{dN}{dD} \propto D^{-2}$ *(—) obtained by the correlation of the velocities between two neighboring sensors inside several flows, a method developed by (Bouchet, 2003).*

Dense flows of grains without cohesion and without interstitial fluid were studied in depth during the last two decades and a general knowledge of their rheological properties under various flow conditions has begun to emerge (see for example the review of GDR MIDI, 2004).Although there remains some debate, da Cruz *et al.* (2005) showed that the behavior of monodisperse granular materials in simple shear at moderate velocities is well described with the help of a frictional law, i.e. $\tau = \mu^* P$, in which

$$\mu^* \approx \mu_s^* + b\dot{\gamma}d\sqrt{\rho_p/P}, \tag{3}$$

d is the diameter of grains, ρ_p their density, and μ_s^* and b are two parameters which depend on the grains properties. This constitutive law corresponds to a yield stress fluid whose apparent viscosity is proportional to $d\sqrt{P}$.

It was shown that, when flowing over a rough inclined plane, granular flows exhibit the same flow regimes as snow: they are steady and uniform in a wide range of slopes, above which they accelerate and below which they decelerate and stop. For steady uniform flows, the stress distribution is of the hydrostatic type as long as the solid fraction is constant. As a consequence the effective friction coefficient μ^* is simply related to the slope: $\mu^*(z) = \tan\theta$ and is constant. Integrating equation (3) we thus find the following shear rate distribution, equivalent to the one obtained with the Norem's Rheology (Norem *et al.*, 1987):

$$\dot{\gamma}(z) \propto \frac{\tan\theta - \mu_s^*}{d}\sqrt{(H-z)\cos\theta}. \tag{4}$$

Such a behavior is sufficient to qualitatively predicts the behavior of each layers when considering that they are made of different size of grains. Let us consider that the bottom layers of snow flow is made of single snow grains (d≈0.4 mm). Then the granular behavior (4) well predicts the behavior of this layer, i.e. the increase of the shear rate $\dot{\gamma}_b$ with both the slope θ and the flow depth H. Let us now consider that the size of grains in the upper layer is given by the size of aggregates (d≈cm). Since the granular behavior (4) predicts that the shear rate scales with the inverse of the grain size: $\dot{\gamma} \propto 1/d$ (Rognon *et al.*,

2007), it well predicts the drop of one order of magnitude of the shear rate between the two layers. Last, we expect that the flow thickness limits the maximal size of the aggregates in the upper layer. We thus may consider that the tipical size of grains in this layer increases when H is increased. Then granular behavior (4) predicts the surpinzing decrease of the shear rate in this layer ($\dot{\gamma}_u$) for an increase of the flow depth H.

Despite this qualitative agreement, fitting the snow velocity profile by (4) requires to overcome two additional difficulties. First, this asks to determine the evolution of the typical diameter of grains along the flow depth which certainly evolves through the upper layer, as suggested in (Rognon *et al.*, 2007). Then, this asks to understand the effect of the rough bottom on the behavior of snow in the first bottom layer. It was shown that the constitutive frictional law (3) does not describe granular flow near the wall. The perturbation due to the basal roughness is still not completely understood, but da Cruz *et al.* (2005); Rognon *et al.* (2007) pointed out an increases of the shear rate in a region thick of approximately five grains. In our snow flow, this would correspond to a basal layer thick of about one millimeter where the shear rate would be strongly increased, thereby favoring sliding velocity.

6 Conclusion

In this paper we investigate the rheological behavior of dense flow of dry snow through in-situ chute flow experiments. Despite strong experimental difficulties, extensive series of steady flows were performed allowing to explore large ranges of slope and flow discharge. This unique data base enabled us to point out new insights into the rheology of dry snow.

The most surprising observation is that the characteristics of flows performed at different periods over three years are remarkably consistent. This enables to identify some generic rheological properties of dry snow without taking into account the variation of snow grains properties due to the continuous snow metamorphism. We first identify three flow regimes as function of the slope: flow are decelerated below about 33°, accelerated above about 41°, and uniform in between these two limits. The mean velocity of the flow is mostly constant around 4 ms^{-1} for any uniform flow, but abruptly drops to zero when approaching to the critical slope 33°. Such an evolution differs from the one of simple yield stress fluids, but is reminiscent to the behavior of granular materials. We then analyse the velocity profiles within uniform snow flows which are found to exhibit a typical type shape: strongly sheared in a thin basal layer and much less sheared in the thick top layer. The drop of the shear rate at the interface whereas stresses slightly vary indicates that the constitutive law of snow must be different in each layers. We interpret this heterogeneity as a consequence of a shear-induced evolution of snow microstructure which gives rise to different materials between the lower and the upper parts of the flow. Our interpretation is that snow flow is initially made of an well mixed mixture of single grains and aggregates, but solid bridges between grains cannot resist in the lower regions submitted to larger stresses combined with the grinding process of the basal roughness. There thereby develops a basal layer of single grains whereas the aggregates are not broken in the upper parts. Moreover, with cohesive grains such as snow ones, sintering can occur at low shear rate which would enhance the heterogeneity of the materials between layers: new bridges can form in the slowly sheared upper part, but cannot form in the rapidly sheared lower part. This structuration - a highly viscous basal layer ensuring fast motion of the solid like upper region which represents most of the material volume- is reminiscent to a caterpillar and should contribute to the potential of snow avalanche to destroy obstacles such as dams or breaking mounds.

The recent advances about the constitutive law describing dense flow of cohesionless grains seems to confirm this interpretation of a two-layered flow. Although granular rheology is still matter of debate, it was shown that the apparent viscosity of the material is proportional to the size of the grains. This constitutive law predicts to a strong difference of shear rate between the basal layer of single grains and the upper layer made of aggregate, and it also qualitatively predicts the behavior which we measured in each layer. However, a quantitative descrition of the snow velocity profiles using granular behavior

requires further studies to understand how the aggregates are distributed along the flow depth, and how the flow is affected near the basal roughness. Nevertheless, these results support the approaches consisting in modeling snow behavior using experimental granular flows. They also points out the crucial role of intergranular cohesive forces into snow behavior through the formation of aggregates within flow, and therefor suggest that experiment with cohesive grains such as wet grass beads or powders, or with polydispersed grains would be more accurate to model dense snow flow.

This study focused on dense flow of dry snow, but few experiments were performed using wet or fresh snow. In both cases, flows stop into the channel even when slope is increases up to 45° (maximum value allowed by the set-up). This difference asks for further studies of the behavior of wet and fresh snow, which are often involved in real avalanches. Another field of investigation is the understating of the fluidization process that we observe at the surface of accelerated flow. It seems to be the first stage of the development of powder avalanches, whose behavior is also a promising field of research.

Acknowledgments

Many people took part in the experimentations, shoveling packed snow up to midnight at 2800m a.s.l., freezing both fingers and toes and sleeping in a small, uncomfortable hut. Their work experience and their enthusiasm were crucial for coping with lots of last-minute hitches, and to successfully carry out experimentation in difficult conditions. We gratefully thank Xavier Ravanat, Gérémie Robert, Sarah Xuereb, Chloée Bois, Michaë Bächer and François-Xavier Cierco for their crucial help in this hard work. We wish to thank Thierry Faug and Guillaume Chambon for interesting discussions at various stages of this study. This work was supported by the E.U. project SATSIE (EVG1-CT2002-00059).

A Discharge equation and constitutive law

We consider a steady and uniform flow down a slope (mean velocity U and thickness H), and we want to demonstrate how the evolution of flow discharge Q can be related to the local constitutive law of the materials. Under the assumption that the sliding velocity is null, the velocity profile is given by an integration of the shear rate profile: $V_x(z) = \int_0^z \dot{\gamma}(\xi; H)d\xi$, where the shear rate $\dot{\gamma}(\xi; H)$ depends on the vertical position ξ as well as on the flow thickness H. The flow rate per unit of with is given by a second integration: $Q = UH = \int_0^H \left[\int_0^z \dot{\gamma}(\xi; H)d\xi\right] dz$. Using an integration by part, the flow rate can be expressed in the following way: $Q = \int_0^H \left[\dot{\gamma}(\xi; H)(H - \xi)\right] d\xi$. Then, tacking the partial derivative of $Q = HU$ with respect to H leads to:

$$\begin{aligned} \frac{\partial Q}{\partial H} &= \int_0^H \frac{\partial}{\partial H}\left[\dot{\gamma}(\xi; H)(H - \xi)\right] d\xi \\ &= \int_0^H \left[\dot{\gamma}(\xi; H) + (H - \xi)\frac{\partial \dot{\gamma}(\xi; H)}{\partial H}\right] d\xi \end{aligned}$$

The intergration of the first term is the velocity at the free surface, $V_x(H)$. In the second term, the partial derivative of the shear with resect to H rate can be replaced by its the partial derivative of the shear with resect to ξ using the following relationship:

$$\frac{\partial \dot{\gamma}(\xi; H)}{\partial H} = -\frac{\partial \dot{\gamma}(\xi; H)}{\partial \xi},$$

which means that adding a little more overbuden has the same effect on the stresses and thus on the shear rate as moving deeper into the flow. Then, the partial derivative of $Q = HU$ with respect to H can be expressed as:

$$\begin{aligned}\frac{\partial Q}{\partial H} &= V_x(H) - \int_0^H \left[(H-\xi)\frac{\partial \dot\gamma(\xi;H)}{\partial \xi}\right] d\xi \\ &= V_x(H) - H(\dot\gamma(H;H) - \dot\gamma(0;H)) + \int_0^H \left[\xi\frac{\partial \dot\gamma(\xi;H)}{\partial \xi}\right] d\xi \\ &= H\dot\gamma(0;H)\end{aligned}$$

after a partial intergation. The advantage of steady and uniform flow regime is that the basal shear stress τ_b is known since it balances the shear stress due to gravity: $\tau_b = \bar\rho g H \sin\theta$. As a consequence, the constitutive law of the materials $\dot\gamma(\tau_b) = \dot\gamma(0;H)$ is given by the variation of the flow discharge Q as function of the flow thickness H, keeping the slope angle θ constant:

$$\dot\gamma(\tau_g) = \frac{1}{H}\left.\frac{\partial (UH)}{\partial H}\right|_\theta .$$

B Linear stability

Let us assume for the sake of simplicity that a constant (apparent) shear rate $\dot\gamma$ is imposed on the material. Thus the velocity under stable conditions is $v_0(z) = \dot\gamma z$. We now assume that the velocity field is slightly perturbed so that its expression becomes $v(z) = v_0(z) + v_1 \exp(ikz + \omega t)$, in which k and ω are two (real) parameters and v_1 is small compared to v_0. Under these conditions, assuming negligible gravity and normal stress effects, the momentum equation along the flow direction reduces to $\rho\frac{\partial v(z)}{\partial t} = \frac{\partial \tau}{\partial z}$. Since we can write $\frac{\partial \tau}{\partial z} = \frac{\partial \dot\gamma}{\partial z}\frac{\partial \tau}{\partial \dot\gamma} = \frac{\partial^2 v}{\partial z^2}\frac{\partial \tau}{\partial \dot\gamma}$, the momentum equation becomes: $\rho\omega = -k^2\frac{\partial \tau}{\partial \dot\gamma}$. This implies that if τ decreases when $\dot\gamma$ increases, ω is positive, which means that the amplitude of the perturbation, proportional to $\exp(\omega t)$, constantly increases in time. Since a real perturbation (of any form) can be decomposed as the sum of an infinity of sinusoidal perturbations of the above form, each of them leading to flow instability, the flow is unstable. When such a constitutive equation (with decreasing stress) is observed in practice it necessarily reflects a localization of shear in a thickness of the order of few diameters of material elements, and the apparent behavior in fact reflects the local behavior of this thin layer for which the validity of the continuum assumption is doubtful.

References

Astarita, G., Marrucci, G. & Palumbo, G. 1964 Non-Newtonian gravity flow along inclined plane surfaces. *Ind. Eng. Chem. Fundam.* **3**, 333–339.

Barbolini, M., Biancardi, A., Cappabianca, F., Natale, L. & Pagliardi, M. 2005*a* Laboratory study of erosion processes in snow avalanches. *Cold Regions Sciences and Technology* **43**, 1–9.

Barbolini, M., Biancardi, A., Natale, L. & Pagliardi, M. 2005*b* A low cost system for the estimation of concentration and velocity profiles in rapid dry granular flows. *Cold Regions Sciences and Technology* **43**, 49–61.

Bouchet, A. 2003 Etude expérimentale des avalanches denses de neige sèche. PhD thesis, Universitée Joseph Fourier, Grenoble, France, in French.

Bouchet, A., Naaim, M., Bellot, H. & Ousset, F. 2004 Experimental study of dense snow avalanches: velocity profiles in steady and fully developed flows. *Annals Glaciology* **49**, 30–34.

Bouchet, A., Naaim, M., Ousset, F., Bellot, H. & Cauvard, D. 2003 Experimental determination of constitutive equations for dense and dry avalanches: presentation of the set-up and first results. *Surveys in Geophysics* **24**, 525–541.

Bridges, F.G., Hatzes, A. & Lin, D.N.C. 1984 Structure, stability and evolution of Saturn's rings. *Nature* **309**, 333–335.

Brown, R.L., Satyawali, P.K., Lehning, M. & Bartelt, P. 2001 Modeling the changes in microstructure of snow during metamorphism. *Cold Regions Sciences and Technology* **33**, 91–101.

Colbeck, S.C. 1983 Theory of metamorphism of dry snow. *J. Geophys. Res.* **88**, 5475–5482.

Colbeck, S.C. 1998 Sintering of a dry snow cover. *J. Appl. Phys.* **84**, 4585–4589.

Coussot, P. 2005 *Rheometry of pastes, suspensions and granular materials*. New York: Wiley.

Coussot, P., Nguyen, Q.D., Huynh, H.T. & Bonn, D. 2002 Viscosity bifurcation in thixotropic, yielding fluids. *J. Rheol.* **43** (3), 1–17.

da Cruz, F., Emam, S., Prochnow, M., Roux, J-N. & Chevoir, F. 2005 Rheophysics of dense granular materials : Discrete simulation of plane shear flows. *Phys. Rev. E* **72**, 021309.

Dent, J. D., Burrell, K. J., Schmidt, D. S., Louge, M. Y., Adams, E. E. & Jazbutis, T. G. 1998 Density, velocity and friction measurement in a dry-snow avalanches. *J. Glaciology* **26**, 247–252.

Dent, J. D. & Lang, T.E. 1983 A biviscous modified Bingham model of snow avalanche motion. *Annals Glaciology* **4**, 42–46.

Faug, T., Naaim, M. & Fourriére, A. 2007 Dense snow flowing past a deflecting obstacle: an experimental investigation. *Cold Regions Sciences and Technology* **49**, 64–73.

Fillot, N., Iordanoff, I. & Berthier, Y. 2004 A granular dynamic model for the degradation of material. *J. Tribology* **126**, 606–614.

Gaméda, S., Vigneault, C. & Raghavan, V. 1996 Snow behaviour under compaction for the production of ice. *Energy* **21**, 15–20.

GDR MIDI 2004 On dense granular flows. *Euro. Phys. J. E* **14**, 341–365.

Gubler, H. 1987 Measurements and modelling of snow avalanche speeds. In *Avalanches Formation, Movement and Effects* (ed. B. Salm & H. Bubler), pp. 405–420. IASH Press, Institute of Hydrology, Wallingford, Oxfordshire, UK: IASH.

Haenel, R.B. & Shoop, S.A. 2004 A macroscale model for low density snow subjected to rapid loading. *Cold Regions Sciences and Technology* **40**, 193–211.

Hatzes, A.P., Bridges, F. & Lin, D.N.C. 1988 Collisional properties of ice spheres at low impact velocity. *Mon. Not. R. Astron. Soc.* **231**, 1091–1115.

Hatzes, A.P., Briges, F., Lin, D.N.C. & Sachtjen, S. 1991 Coagulation of particules in Saturn's rings: Measurements of the cohesive force of water frost. *Icarus* **89**, 113–121.

Higa, M., Arakawa, M. & Maeno, N. 1995 Measurements of restitution coefficients of ice at low temperatures. *Planet. Space. Sci.* **44**, 917–925.

Johnson, J.B. & Schneebeli, M. 1999 Characterizing the microstructural and micromechanical properties of snow. *Cold Regions Sciences and Technology* **30**, 91–100.

Jop, P., Forterre, Y. & Pouliquen, O. 2005 Crucial role of sidewalls in dense granular flows: consequence on the rheology. *J. Fluid Mech.* **541**, 167–192.

Kern, M.A., Tiefenbacher, F. & McElwaine, J.N. 2004 The rheology of snow in large chute flows. *Cold Regions Sciences and Technology* **39**, 181–192.

Khosropour, R., Zirinsky, Jessie, Pak, H. K. & Behringer, R. P. 1997 Convection and size segregation in a couette flow of granular material. *Phys. Rev. E* **56** (4), 4467–4473.

Kry, P.R. 1975 The relationship between the visco-elastic and structural properties of fine-grained snow. *J. Glaciology* **14**, 479–500.

Kuroiwa, D. 1974 Metamorphism of snow and ice sintering observed by time lapse cine-photomicrography. In *Snow Mechanics Symposium* (ed. A. A. Balkema), pp. 82–88. Washington, D.C.: International Association of Hydrological Sciences.

Lehing, M., Bartelt, P., Brown, B., Fierz, C. & Satyawali, P. 2002 A physical SNOWPACK model for the Swiss avalanche warming Part II. Snow microstructure. *Cold Regions Sciences and Technology* **35**, 147–167.

Louge, M.Y. & Keast, S.C. 2001 On dense granular flows down flat frictional inclines. *Phys. Fluids* **13**, 1213–1233.

Mangeney, A., Vilotte, J-P., Bristeau, M-O., Perthame, B., Simeoni, C. & Yerneni, S. 2003 Numerical modelling of avalanches based on saint venant equations using a kinetic scheme. *J. Geophys. Res.* In press.

Marbouty, D. 1980 An experimental study of temperature-gradient metamorphism. *J. Rheol.* **26**, 303–311.

Meunier, M., Taillandier, J.M. & Ancey, C. 2004 Fitting avalanche-dynamics models with documented events from the Col du Lautaret site (France) using the conceptual approach. *Cold Regions Sciences and Technology* **39**, 55–66.

Naaim, M. & Naaim-Bouvet, F., ed. 2001 *Snow and avalanches test sites*. Cemagref Editions.

Naaim, M., Naaim-Bouvet, F., Faug, T. & Bouchet, A. 2004 Dense snow avalanche modeling: flow, erosion, deposition and obstacle effects. *Cold Regions Sciences and Technology* **39**, 193–204.

Naaim, M., Vial, S. & Couture, R. 1997 St Venant approach for rock avalanches modelling in multiple scale analysis and coupled physical systems. In *St Venant symposium* (ed. Presse de l'Ecole Nationale des Ponts et Chaussées). Paris.

Nakaya, U. 1954 *Snow crystals: Natural and Artificial*. Boston, U.S.A.: Harvard University Press.

Nishimura, K. & Maeno, N. 1989 Contribution of viscous forces to avalanche dynamics. *Annals Glaciology* **13**, 202–206.

Norem, H., Irgens, F. & Schieldrop, B. 1987 A continum model to calculate snow-avalanche velocity. *International Association of Hydrological Sciences Publication* **162**, 363–379.

Pouliquen, O. 1999 Scaling laws in granular flows down a rough inclined plane. *Phys. Fluids* **11**, 542–548.

Pouliquen, O. & Chevoir, F. 2002 Dense flows of dry granular materials. *Compte Rendu Physique* **3**, 163–175.

Qiu, J., Xu, J. & Jiang, F. 1997 Study of avalanches in the Tianshan Montains, Xinjiang, China. *Snow Engineering:Recent Advances* .

Rastello07, M. & Bouchet, A. 2007 Surface oscillations in channeled snow flows. *Cold Regions Sciences and Technology* **49**, 134–144.

Reiter, C.A. 2005 A local cellular model for snow crystal growth. *Chaos, Solitons and Fractals* **23**, 1111–1119.

Rognon, P. 2006 Rheology of cohesive granular materials, application to dense snow avalanches. PhD thesis, Ecole Nationale des Ponts et Chaussées, Paris, in French.

Rognon, P. G., Roux, J-N., Naaim, M. & Chevoir, F. 2007 Dense flows of bidisperse assemblies of disks down an inclined plane. *Phys. Fluids* **19**, 058101.

Rognon, P. G., Roux, J-N., Wolf, D., Naaim, M. & Chevoir, F. 2006 Rheophysics of cohesive granular materials. *Europhys. Lett.* **74**, 644–650.

Savage, S.B. & Lun, C.K.K. 1988 Particle size segregation in inclined chute flow of dry cohesionless granular solids. *J. Fluid Mech.* **189**, 311–335.

Savage, S. B. 1979 Gravity flow of cohesionless granular materials in chutes and channels. *J. Fluid Mech.* **92**, 53–96.

Savage, S. B. & Hutter, K. 1989 The motion of a finite mass of granular material down a rough inclined. *J. Fluid Mech.* **199**, 177.

Schweizer, J. & Camponovo, C. 2001 The temperature dependence of the effective elastic shear modulus of snow. *Cold Regions Sciences and Technology* **35**, 55–64.

St Lawrence, W. & Bradley, C.C. 1974 The deformation of snow in terms of structural mechanism. In *Snow Mechanics Symposium*, pp. 155–169. A. A. Balkema.

Supulver, K.D., Bridges, F.G. & Lin, D.N.C. 1995 The coefficient of restitution of ice particules in glancing collisions: experimental results for unfrosted surfaces. *Icarus* **113**, 188–199.

Tiefenbacher, F. & Kern, M.A. 2004 Experimental devices to determine snow avalanche basal friction and velocity profiles. *Cold Regions Sciences and Technology* **38**, 17–30.

Vallet, J., Gruber, U. & Dufour, F. 2001 Photogrametric avalanche measurements at Vallée de la Sionne, Switzerland. *Annals Glaciology* **32**, 141–146.

Voitkovsky, K.F., Bozhinsky, A.N., Gobulev, V.N., Laptev, M.N., Zhigulsky, A.A. & Slesarenko, Y.Y. 1974 Creep-induced changes in structure and density of snow. In *Snow Mechanics Symposium*, pp. 171–179. A. A. Balkema.